Multiphase flow and bubble size distribution in continuous casters using a hybrid EEDPM model

YANG Hyunjin[1] and THOMAS, Brian G.[2]

1. Department of Mechanical Science and Engineering, University of Illinois at Urbana-Champaign, 1206 W. Green Street, Urbana, IL 61801 USA

2. Department of Mechanical Engineering, Colorado School of Mines, Brown Hall W370-B, 1610 Illinois Street, Golden, CO 80401 USA

Abstract: In the continuous casting process, argon gas injection can help to avoid nozzle clogging and to remove impurities, but it causes complexity associated with turbulent multiphase flow. In particular, the actual bubble size distribution in the mold remains unclear, even though it has a great influence on the flow pattern and the generation of defects. In this study, a new computational model has been developed in order to simulate the fluid flow and bubble size distribution in continuous casting. This hybrid model of multiphase flow and bubble size distribution combines together simultaneously, a Eulerian Eulerian model (EE) coupled with a Discrete Phase Model (DPM), called EEDPM. Large gas pockets are simulated directly by the Eulerian Eulerian model, and smaller bubbles are tracked by the Discrete Phase Model. Another model is implemented to predict the shearing-off process to calculate the number, sizes and frequency of bubbles that detach from the large gas pockets, and are then injected as Discrete Phase Model bubbles. The local, time-varying bubble sizes from the DPM are input to the EE model for a local momentum-exchange interaction. This hybrid model is validated by comparison with measurements in a lab-scale experiment[1].

Key words: multiphase flow, bubble size distribution, Eulerian Eulerian model, Discrete Phase model, shearing off

In continuous casting of steel, multiphase flow is due to argon gas injection into the upper tundish nozzle (UTN) to reduce nozzle clogging[2,3]. The injected argon gas interacts with the liquid steel flow in a complex manner to produce a size distribution of bubbles exiting the nozzle into the mold. This bubble size distribution is a key factor to analyse flow pattern and surface level behaviour in the mold, which is directly related to defect mechanisms and quality of the final product.

Determination of the actual bubble size distribution is very difficult, owing to the complex nature of multiphase flow and lack of proper models to simulate all of the governing phenomena. Furthermore, the measurement of bubble sizes in real commercial casters is equally difficult. Recently, Timmel et al[1] visualized the behaviour of argon bubbles and liquid metal in a lab-scale stopper-rod system using X-ray. The bubble size distribution in the mold is a consequence of four steps: 1) generation of recirculation zones in the flow near the stopper rod, 2) formation of gas pockets by accumulation of bubbles in the recirculation zones[4], 3) bubble detachment from the gas pockets by a shearing off process[7,8], and 4) bubble interactions (coalescence and breakup)[10-12] as the flow continues down the nozzle. To estimate the evolution of bubble size distribution, a multiphase flow model must capture all these steps properly. In this paper, a new hybrid model which couples a Eulerian-Eulerian model (EE)[5] with a Discrete Phase Model (DPM)[6], called EEDPM, is introduced, to estimate the evolution of bubble size distribution in the continuous casting system.

1. Model description

1.1 Governing equations

As its name suggests, the hybrid model (EEDPM) consists of: EE model[5] (Eq 1~3) and DPM[6] (Eq 4~5).

$$\frac{\partial(\alpha_k\rho_k)}{\partial t} + \nabla\cdot(\alpha_k\rho_k\boldsymbol{u}_k) = 0 \quad (1)$$

$$\frac{\partial(\alpha_k\rho_k\boldsymbol{u}_k)}{\partial t} + \nabla\cdot(\alpha_k\rho_k\boldsymbol{u}_k\boldsymbol{u}_k) = -\alpha_k\nabla p + \nabla\cdot(\mu_k\alpha_k(\nabla\boldsymbol{u}_k + \nabla\boldsymbol{u}_k{}^T)) + \alpha_k\rho_k\boldsymbol{g} + K_{kq}(\boldsymbol{u}_k - \boldsymbol{u}_q) \quad (2)$$

$$K_{kq} = \frac{3}{4}\frac{C_D}{d}\alpha_q(1-\alpha_q)\rho_k|\boldsymbol{u_k} - \boldsymbol{u_q}|,\ K_{kq} = K_{qk} \quad (3)$$

$$m_b\frac{d\boldsymbol{v}_i}{dt} = \sum\boldsymbol{F} = \boldsymbol{F}_D + \boldsymbol{F}_V + \boldsymbol{F}_B + \boldsymbol{F}_P \quad (4)$$

$$\boldsymbol{r_{i,2}} = \boldsymbol{r_{i,1}} + \int_0^t \boldsymbol{v}_i\,dt \quad (5)$$

The EE model simulates the flow pattern including the gas pockets, while the DPM model tracks sheared off bubbles from the gas pockets, to provide the bubble size distribution and local interface area back to the EE

model, needed to calculate momentum interaction (Eq. 3). The DPM bubbles are coupled with the EE model results, as the liquid velocity determines the forces acting on the gas bubbles, affecting their trajectories. In turn, the local and time-varying DPM bubble information enables the EE model to calculate better velocity and void fraction fields than a classic EE model with a prefixed bubble size in time and space.

1.2 Shearing off model

To simulate the detachment of small bubbles from gas pockets, a new shearing-off model has been developed. This model starts with the velocity and gas volume fraction fields from the EE model. The interface of the large gas pockets is then identified, through an approximation process, based simply in this initial work on choosing the 95% gas volume fraction contour ($\alpha^* = 1 \ if \ \alpha \geq 0.95, otherwise \ 0$). After the gas pockets and their interfaces are obtained, the interface area and detachment points of small bubbles are calculated for each pocket. The detachment point is estimated as the lowest point of the gas pocket (in downward flow). Then, the volume that is sheared-off from the gas pocket is calculated by multiplying the interface area by the thickness of the detached layer ($V_{so} = A_{int}\delta_g^*$). The sheared-off gas layer thickness (δ_g^*) is calculated from boundary layer theory[7,8]. Next, this sheared-off volume is distributed into small bubbles. According to previous work from bubble breakup experiments, the daughter bubble size from breakage is treated as a stochastic variable[9,10]. This size is chosen randomly within a range defined using several criteria based on mass, momentum and energy balances. Specifically, based on the criteria of Luo and Svendsen (1996) [10] and Wang et al. (2003) [11], energy and force criteria are derived for the minimum and maximum bubble sizes, while a third mass conservation criterion is applied to keep the total volume of daughter bubbles within the total sheared-off volume from the gas pocket.

$$d_{min} = \frac{2\sigma}{0.5\rho_l u_l^2 - \sum_{i=1}^{N} \frac{\pi\sigma d_{di}^2}{V_{lf}}} \quad (6)$$

$$d_{m,max} = \left(\frac{V_{so} - \sum_{i=1}^{N} \frac{1}{6}\pi d_{di}^3}{\frac{1}{6}\pi} \right)^{\frac{1}{3}} \quad (7)$$

$$d_{e,max} = \sqrt{\frac{0.5\rho_l u_l^2 V_{lf} - \sum_{i=1}^{N} \pi\sigma d_{di}^2}{\pi\sigma}} \quad (8)$$

The force criterion generates the lower bound (d_{min}), and the mass and energy criteria generate two upper bounds of bubble size ($d_{m,max}, d_{e,max}$). The bubbles must satisfy all three criteria, so the smaller upper bound is chosen for the final upper bound. A daughter bubble size is chosen through a random generator within the range of bounds, and injected at the detachment point as a Discrete Phase Model (DPM) bubble. The upper and lower bounds evolve as each daughter bubble detaches: the mass, momentum and energy are consumed from the total volume, momentum and energy of the sheared-off liquid film of the gas pocket. As bubbles detach, the lower bound increases and upper bounds decrease. When the upper bound becomes less than the lower bound, that period of the shearing-off breakup process ends. The frequency of shearing-off processes is estimated from the time period taken to replenish the gas pocket, found by dividing the gas pocket length by the liquid velocity surrounding it.

1.3 Change of bubble volume by liquid pressure

Gas bubbles can expand or shrink based on the surrounding liquid pressure. The local bubble size is calculated according to the local liquid pressure, by solving the following cubic equation for r_2 (bubble radius at new position 2), which was derived from the Young-Laplace equation and the ideal gas law:

$$p_{l2} r_2^3 + 2\sigma r_2^2 - p_{g1} r_1^3 = 0 \quad (9)$$

By solving this equation transiently for each DPM bubble, gas volume change by liquid pressure is captured appropriately.

2. Simulation results

2.1 Numerical setup

The EEDPM hybrid model is applied to simulate the relevant benchmark experiment of Timmel[1] as an example validation problem. As shown in Figure 1, liquid Galinstan metal flows through a slot-shaped geometry that is 12mm thick. Liquid enters the top of the funnel shape and flows downward by gravity. Argon gas is injected from the tip of the rectangular stopper rod. Boundary conditions shown in Figure 1 are defined based on the operating conditions given in Table 1. The simulation is operated using ANSYS-Fluent with extensive UDF user subroutines. The standard k-ε model is used for the turbulence model. The mesh has 0.6 million hexahedral cells. The simulation lasts for 7

seconds from a EE model steady state solution and the time step size is chosen fixed at 0.001 second.

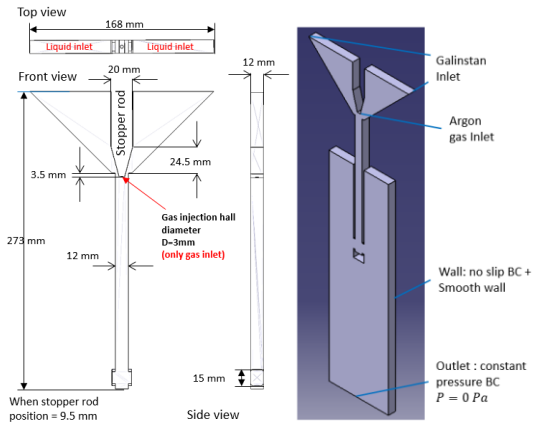

Figure 1. Schematic of the geometry[1]

Table 1. (below) Liquid and gas flow rate conditions

Operating condition	**Value**
Operating temperature	293K
Stopper rod position	19mm
Tundish level	70mm
Galinstan flow rate	115 cm^3/s (condition1) 140 cm^3/s (condition2)
Argon gas flow rate	1.7 cm^3/s (condition1) 0.24 cm^3/s (condition2)
Submergence depth	92mm
Wall roughness	smooth wall (acrylic)
Gas volume fraction	1.4% (condition1) 0.2% (condition2)
Material property	**Value**
Galinstan density	6440 kg/s
Galinstan viscosity	0.0024 Pa
Galinstan surface tension coefficient	0.718 N/m
Argon gas density	1.6228 kg/m^3
Argon gas viscosity	2.125×10^{-5} Pas

2.2 Simulation results

Figure 2 shows a comparison of gas pocket shape between the hybrid model simulation and the lab experiment x-ray visualization [1] for condition 1.

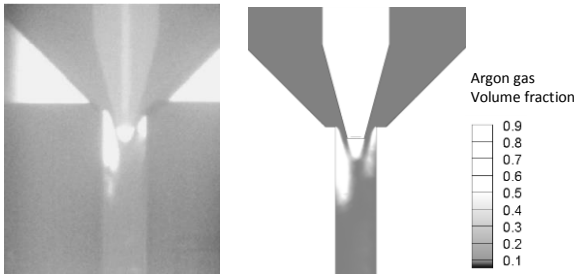

Figure 2. Comparison of measurement (left) and simulation result (right) for the gas pocket shape

The simulation and measured results both show that three gas pockets form: at the stopper tip and side walls. A periodic oscillation of the gas pockets coupled with velocity field is observed in both results. Furthermore, the gas pockets are osbserved to shed bubbles periodically. Figure 3 shows the velocity, void fraction and DPM bubbles from the EEDPM simulation near the inlet of the SEN for condition 2. The model DPM bubbles are observed to start at the bottom of the two side gas pockets of the EE model, according to the shearing-off model.

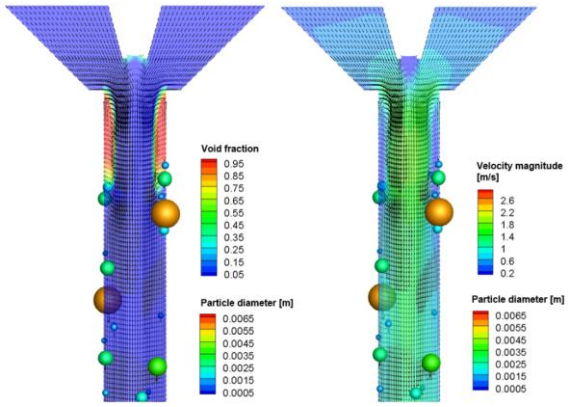

Figure 3. Transient flow pattern and void fraction field of EEDPM simulation at 7 second

Figure 4 shows the distribution of the DPM bubbles generated by the model, which then flow down the nozzle to enter the mold cavity. The number of bubbles in the nozzle and mold are shown separately and the local Sauter-mean average bubble sizes are calculated in each zone, and range from 2.4 to 5.3mm. The trend in size evolution between zones is not consistent because insufficient time has elapsed to gather enough statistics.

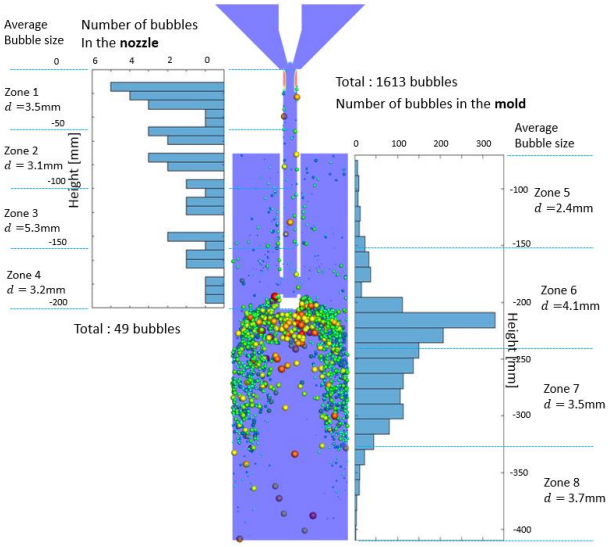

Figure 4. Distribution of DPM bubbles and local Sauter-mean averages of bubble diameters at 7 second

The majority of bubbles in the mold region are found in the lower part of the mold below the nozzle. The strong

jet from the port impinges onto the mold wall and divides upwards and downwards. Bubbles entrained with the upward flow can escape from the top surface of the mold, so only a few are observed. Bubbles entrained with the downward flow are mostly trapped beneath the jet, because the jet obstructs their path to float upwards. Some bubbles escape through the bottom of the mold, but most of them are accumulate below the jet and circulate in the lower region of the mold. The experimental observations report the same phenomenon that only a few bubbles rise directly toward the top surface, and most bubbles are found in the lower region of the mold below the nozzle port. Figure 5 shows the bubble size distrubution from EEDPM model, and Figure 6 compares these results to the measurements. The trend matches well, but the simulation slightly overestimates the bubble size.

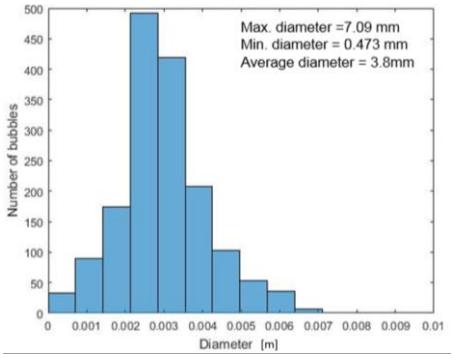

Figure 5. Size distribution of DPM bubbles

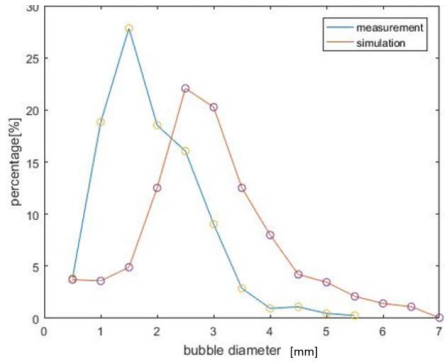

Figure 6. Comparison of bubble size distribution to the measurement

3. Conclusions

In this study, a new hybrid model EEDPM is presented to simulate multiphase flow in steel continuous casting with argon gas, featuring an estimation of bubble size distribution evoluation. This model is able to simulate three of the four steps of bubble size formation (generation of recirculation zones, formation of gas pockets and shearing off process). The bubble size distribution resulting from these steps shows a typical Rosin-Rammler size distribution, and shows a similar trend to the measurements. We expect better accuracy when the hybrid model is improved with bubble interactions, such as bubble breakup, which should shift the distribution to smaller sizes. Finally, it is important to mention that the geometry of the test system studied in this work is much smaller, thinner, and rectangular compared with the real commercial-casting stopper-rod nozzle and caster system. The flow and argon gas behavior is expected to be very different in the real system, and will be the subject of future work.

Nomenclature:

<Symbols>

A_{int}: interface area of gas pocket, C_D: drag coefficient,
d: diameter of a bubble, $\boldsymbol{F}$: force, $\boldsymbol{g}$: gravity,
K_{kq}: momentum transfer coefficient from phase k to phase q, m_b: mass of a bubble, p: pressure,
$\boldsymbol{r}$: DPM bubble position, r: bubble radius, t: time,
$\boldsymbol{u}$: velocity field, u: velocity magnitude
$\boldsymbol{v_i}$: i-th DPM bubble velocity, V: volume
α: EE volume fraction field, α^*: approximated volume fraction field, μ: viscosity, ρ: density, σ: surface tension coefficient, δ_g^* : sheared off gas layer thickness,
$\sum_{j=1}^{N}$: summation of sheared off bubbles created in one shearing off process

<Subscripts>

k and q: arbitrary phase (gas or liquid), D: drag,
V: virtual mass, B: buoyancy, P: pressure gradient,
SO: sheared off, lf: liquid film, l: liquid, g: gas
1: old position, 2: new position,

References:

[1] Timmel, Klaus, Natalia Shevchenko, Michael Röder, Marc Anderhuber, Pascal Gardin, Sven Eckert, and Gunter Gerbeth. *Metallurgical and Materials Transactions B* 46, no. 2 : 700–710.
[2] Bai, Hua, and Brian G. Thomas. *Metallurgical and Materials Transactions B* 32, no. 6: 1143–59.
[3] Rui, and Brian G. Thomas. *Metallurgical and Materials Transactions B* 46, no. 1: 388–405.
[4] Bai, Hua, and Brian G. Thomas. *Metallurgical and Materials Transactions B* 32, no. 2 : 253–67.
[5] Harlow, Francis H., and Anthony A. Amsden. *Journal of Computational Physics* 17, no. 1 (1975)
[6] Riley, James J. *Physics of Fluids* 17, no. 2 (1974): 292.
[7] Fernandes, R. C., R. Semiat, and A. E. Dukler. *AIChE Journal* 29, no. 6: 981–89.
[8] Fu, X.Y, and M Ishii. *Nuclear Engineering and Design* 219, no. 2: 143–68.
[9] Hesketh, R. P., T. W. Fraser Russell, and A. W. Etchells. *AIChE Journal* 33, no. 4: 663–67.
[10] Luo, Hean, and Hallvard F. Svendsen *AIChE Journal* 42, no. 5: 1225–33.
[11] Wang, Tiefeng, Jinfu Wang, and Yong Jin. *Chemical Engineering Science* 58, no. 20: 4629–37.
[12] Prince, Michael J., and Harvey W. Blanch. *AIChE Journal* 36, no. 10: 1485–99.